

# A Metric Hybrid Planning Approach to Solving Pandemic Planning Problems with Simple SIR Models

Ari Gestetner, Buser Say

Monash University  
Melbourne, Australia  
ages0001@student.monash.edu, buser.say@monash.edu

## Abstract

A pandemic is the spread of a disease across large regions, and can have devastating costs to the society in terms of health, economic and social. As such, the study of effective pandemic mitigation strategies can yield significant positive impact on the society. A pandemic can be mathematically described using a compartmental model, such as the Susceptible–Infected–Removed (SIR) model. In this paper, we extend the solution equations of the SIR model to a state transition model with lockdowns. We formalize a metric hybrid planning problem based on this state transition model, and solve it using a metric hybrid planner. We improve the runtime effectiveness of the metric hybrid planner with the addition of valid inequalities, and demonstrate the success of our approach both theoretically and experimentally under various challenging settings.

## Introduction

A pandemic is the spread of an infectious disease across large regions, and can incur devastating costs to the society in terms of health, economic and social. A pandemic can be mathematically described as a compartmental model, such as the Susceptible–Infected–Removed (SIR) model. (Kermack and McKendrick 1927; Bailey 1975) The SIR model categorizes each individual in the population into three compartments, namely: either Susceptible, Infected or Removed, and uses a system of partial differential equations (PDEs) to describe the interaction between these compartments. As visualized in figure 1, the purpose of a pandemic planning problem is to find a solution that keeps the number of removed individuals under a certain threshold while also keeping the number of infected individuals under a certain threshold (i.e., without overwhelming the healthcare system) over some duration (e.g., until vaccinations are expected to become available), by deciding on the selection, timing and duration of effective mitigation decisions (e.g., lockdowns).

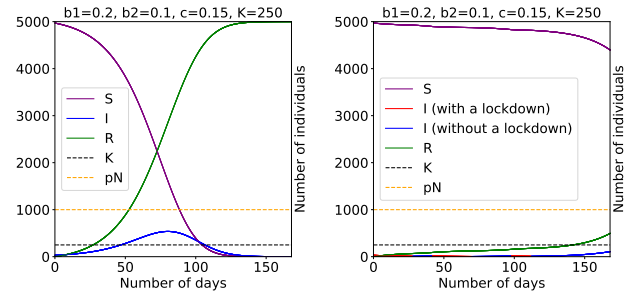


Figure 1: Visualization of two pandemic curves based on the SIR model. The purple curves represent susceptible individuals, blue curves represent the infected individuals when there are no lockdowns and the green curves represent the removed individuals. The goal of pandemic planning problem is to keep the number of removed individuals under a certain threshold (i.e., orange dashed line) while also keeping the number of infected individuals under a certain threshold (i.e., black dashed line). On the left is the visualization of the natural spread of a disease without any lockdowns and on the right is the spread of the same disease under the plan that is produced by SCIPPlan using lockdowns (i.e., red lines).

Automated planning formally reasons about the selection, timing and duration of actions to reach desired states of the world as best as possible. (Nau, Ghallab, and Traverso 2004) Automated planners have significantly improved the ability of autonomous systems to solve challenging tasks such as, traffic control (McCluskey and Vallati 2017), smart grid control (Thiébaut et al. 2013), Heating, Ventilation and Air Conditioning (HVAC) control (Say et al. 2017), and Unmanned Aerial Vehicles (UAV) control (Ramirez et al. 2018). While automated planning has been shown to successfully control many physical systems, the control of pandemics still presents non-trivial challenges to many of the existing automated planners mainly due to the complexity of the underlying system of equations that govern the evolution of the spread of the disease over time, which demands constrained and combinatorial sequential reasoning over PDEs.

A common approach to sequential decision making with a PDE-based model is to discretize the time and approximately update the state of the world with each discrete increment of time. (Morari, Garcia, and Prett 1988; Li and

Williams 2008; Penna et al. 2009; Piotrowski et al. 2016; Scala et al. 2016) The main advantage of this approach is that it allows systems that can be modelled using PDEs with no known solution equations to be approximately controlled. The main disadvantage of this approach is that its accuracy and performance are highly sensitive to the arbitrary choice of the granularity of the time discretization. This can be particularly problematic for systems that exhibit exponential growth behaviour, such as the case in pandemics. An alternative approach here is to work directly with the solution equations of the PDEs. The main advantage of this approach is that it allows for the continuous time control of the underlying system. (Coles et al. 2012; Shin and Davis 2005; Cashmore et al. 2016; Say and Sanner 2019; Chen, Williams, and Fan 2021) The main disadvantage of this approach is that not all PDEs have known solution equations. However, it should be noted that the advancements of machine learning techniques (Raissi, Perdikaris, and Karniadakis 2019; Karniadakis et al. 2021) allow for the accurate approximation of the solution equations of many complex systems of PDEs from (real and/or simulated) data, which makes this disadvantage less consequential in practise.

In this paper, we will solve the pandemic planning problem using an automated planner that is capable of synthesizing plans over continuous time. Specifically, we will begin by building a state transition model based on the solution equations of the SIR model (Bailey 1975; Gleissner 1988; Bohner, Streipert, and Torres 2019) with infection rate that is a function of the lockdown decision. Given the state transition model, we will formalize the pandemic planning problem as a metric hybrid planning problem (Say and Sanner 2019). We will introduce domain-dependent valid inequalities in order to improve the computational effectiveness of the automated planner. We will show theoretical results on the finiteness and the correctness of the automated planner for solving the pandemic planning problem, and experimentally validate the success of our approach under various challenging settings.

## Background

We begin by presenting the definition of the metric hybrid planning problem that will be used to formalize the pandemic planning problem, a metric hybrid planner for solving the pandemic planning problem, and the SIR model that will form the basis of the pandemic planning problem.

### The Metric Hybrid Planning Problem

A *metric hybrid planning problem* (Say and Sanner 2018a, 2019; Say 2023) is defined as a tuple  $\Pi = \langle S, A, \Delta, C^I, C^T, T, V, G, R, H \rangle$  where

- $S = \{s_1, \dots, s_n\}$  is the set of state variables with bounded domains  $D_{s_1}, \dots, D_{s_n}$  for positive integer  $n \in \mathbb{Z}^+$ ,
- $A = \{a_1, \dots, a_m\}$  is the set of action variables with bounded domains  $D_{a_1}, \dots, D_{a_m}$  for positive integer  $m \in \mathbb{Z}^+$ ,
- $\Delta \in [\epsilon, M]$  is the duration of a step for positive real numbers  $\epsilon \in \mathbb{R}^+$  and  $M \in \mathbb{R}^+$  such that  $\epsilon \leq M$ ,

- $C^I : \prod_{i=1}^n D_{s_i} \times \prod_{i=1}^m D_{a_i} \times [\epsilon, M] \rightarrow \mathbb{R}$  is the instantaneous constraint function that is used to define the constraint  $C^I(s_1^t, \dots, s_n^t, a_1^t, \dots, a_m^t, \Delta^t) \leq 0$  for all steps  $t \in \{1, \dots, H\}$ ,
- $C^T : \prod_{i=1}^n D_{s_i} \times \prod_{i=1}^m D_{a_i} \times [\epsilon, M] \rightarrow \mathbb{R}$  is the temporal constraint function that is used to define the constraint  $C^T(s_1^t, \dots, s_n^t, a_1^t, \dots, a_m^t, \Delta^t) \leq 0$  for all steps  $t \in \{1, \dots, H\}$ ,
- $T : \prod_{i=1}^n D_{s_i} \times \prod_{i=1}^m D_{a_i} \times [\epsilon, M] \rightarrow \prod_{i=1}^n D_{s_i}$  is the state transition function,
- $V$  is a tuple of constants  $\langle V_1, \dots, V_n \rangle \in \prod_{i=1}^n D_{s_i}$  denoting the initial values of state variables,
- $G : \prod_{i=1}^n D_{s_i} \rightarrow \mathbb{R}$  is the goal function that is used to define the constraint  $G(s_1^{H+1}, \dots, s_n^{H+1}) \leq 0$ ,
- $R : \prod_{i=1}^n D_{s_i} \times \prod_{i=1}^m D_{a_i} \times [\epsilon, M] \rightarrow \mathbb{R}$  is the reward function, and
- $H \in \mathbb{Z}^+$  is the horizon.

A *solution* to  $\Pi$  is defined as a tuple of values  $\langle \bar{a}_1^t, \dots, \bar{a}_m^t \rangle \in \prod_{i=1}^m D_{a_i}$  for all action variables  $A$  and a value  $\bar{\Delta}^t \in [\epsilon, M]$  for all steps  $t \in \{1, \dots, H\}$  and a tuple of values  $\langle \bar{s}_1^t, \dots, \bar{s}_n^t \rangle \in \prod_{i=1}^n D_{s_i}$  for all state variables  $S$  and steps  $t \in \{1, \dots, H+1\}$  if and only if the following conditions hold:

1.  $\bar{s}_i^1 = V_i$  for all  $i \in \{1, \dots, n\}$ ,
2.  $T(\bar{s}_1^t, \dots, \bar{s}_n^t, \bar{a}_1^t, \dots, \bar{a}_m^t, \bar{\Delta}^t) = \langle \bar{s}_1^{t+1}, \dots, \bar{s}_n^{t+1} \rangle$  for steps  $t \in \{1, \dots, H\}$ ,
3.  $C^I(\bar{s}_1^t, \dots, \bar{s}_n^t, \bar{a}_1^t, \dots, \bar{a}_m^t, \bar{\Delta}^t) \leq 0$  for steps  $t \in \{1, \dots, H\}$ ,
4.  $C^T(\bar{s}_1^t, \dots, \bar{s}_n^t, \bar{a}_1^t, \dots, \bar{a}_m^t, x^t) \leq 0$  for steps  $t \in \{1, \dots, H\}$  and for all values of  $x^t \in [0, \bar{\Delta}^t]$ , and
5.  $G(\bar{s}_1^{H+1}, \dots, \bar{s}_n^{H+1}) \leq 0$ .

Similarly, an *optimal solution* to  $\Pi$  is a solution that also maximizes the reward function  $R$  over the planning horizon  $H$  such that:

$$\max_{\substack{a_1^1, \dots, a_m^H \\ \Delta_1^1, \dots, \Delta_H^1}} \sum_{t=1}^H R(s_1^t, \dots, s_n^t, a_1^t, \dots, a_m^t, \Delta^t)$$

Next, we will present a methodology for solving  $\Pi$ .

### Solving the Metric Hybrid Planning Problem

SCIPPlan (Say and Sanner 2018a, 2019; Say 2023) is a metric hybrid planner that performs on mathematical optimization. SCIPPlan compiles  $\Pi$  into the mathematical optimization model that is provided below.

$$\max_{\substack{a_1^1, \dots, a_m^H \\ \Delta^1, \dots, \Delta^H}} \sum_{t=1}^H R(s_1^t, \dots, s_n^t, a_1^t, \dots, a_m^t, \Delta^t) \quad (1)$$

$$s_i^1 = V_i \quad \forall i \in \{1, \dots, n\} \quad (2)$$

$$T_i(s_1^t, \dots, \Delta^t) = s_i^{t+1} \quad \forall i \in \{1, \dots, n\}, t \in \{1, \dots, H\} \quad (3)$$

$$C^I(s_1^t, \dots, \Delta^t) \leq 0 \quad \forall t \in \{1, \dots, H\} \quad (4)$$

$$C^T(s_1^t, \dots, c^t \Delta^t) \leq 0 \quad \forall c^t \in [0, 1], t \in \{1, \dots, H\} \quad (5)$$

$$G(s_1^{H+1}, \dots, s_n^{H+1}) \leq 0 \quad (6)$$

$$s_i^t \in D_{s_i} \quad \forall i \in \{1, \dots, n\}, t \in \{1, \dots, H+1\} \quad (7)$$

$$a_i^t \in D_{a_i} \quad \forall i \in \{1, \dots, m\}, t \in \{1, \dots, H\} \quad (8)$$

$$\epsilon \leq \Delta^t \leq M \quad \forall t \in \{1, \dots, H\} \quad (9)$$

The brief description of the mathematical optimization model is as follows. The objective function (1) maximizes the total reward accumulated over the horizon. Constraint (2) sets the initial values of all state variables. Constraint (3) sets the values of state variables in the next step given the values of state and action variables in the current step. Constraints (4-6) enforce the instantaneous, temporal and goal constraints. Constraints (7-9) set the domains of state, action and duration variables, respectively. Note that in the mathematical optimization model presented above, constraint (5) is an interval constraint that holds for all values of the interval  $c^t \in [0, 1]$ . SCIPPlan uses a constraint generation framework that iteratively identifies unique violated values of  $c^t \in [0, 1]$  and generates constraint (5) with the identified violated values of  $c^t$ . It has been shown that SCIPPlan terminates either with a solution to  $\Pi$  with at most some constant  $\gamma$  violation of constraint (5) or proves the infeasibility of  $\Pi$  in finite number of constraint generation iterations.<sup>1</sup> Next, we will describe the SIR model that will be used to construct the state transition function  $T$  of our planning problem  $\Pi$ .

## The SIR Model with Constant Infection and Recovery Rates

The SIR model (Kermack and McKendrick 1927) is a compartmental model that groups a population into three compartments, namely: Susceptible, Infected and Removed. The SIR model mathematically describes the interaction between these groups using a system of partial differential equations. In this paper, we will build a state transition function  $T$  based on the solution equations of the SIR model with constant infection  $b \in [0, 1]$  and removal  $c \in [0, 1]$  rates. (Bailey 1975; Gleissner 1988; Bohner, Streipert, and Torres 2019)

<sup>1</sup>The proof assumes the temporal constraint function  $C^T$  to be Lipschitz continuous. Other control functions can be used to derive domain-specific bounds based on the analysis of  $C^T$ , as we will show in section .

The system of partial differential equations:

$$x' = -\frac{bxy}{x+y} \quad (10)$$

$$y' = \frac{bxy}{x+y} - cy \quad (11)$$

$$z' = cy \quad (12)$$

has the following solution equations for  $b \neq c$ :

$$x^{t+1} = x^t \left(1 + \frac{y^t}{x^t}\right)^{\frac{b}{b-c}} \left(1 + \frac{y^t}{x^t} e^{(b-c)\Delta^t}\right)^{-\frac{b}{b-c}} \quad (13)$$

$$y^{t+1} = y^t \left(1 + \frac{y^t}{x^t}\right)^{\frac{b}{b-c}} \left(1 + \frac{y^t}{x^t} e^{(b-c)\Delta^t}\right)^{-\frac{b}{b-c}} e^{(b-c)\Delta^t} \quad (14)$$

$$z^{t+1} = N - (x^t + y^t)^{\frac{b}{b-c}} (x^t + y^t e^{(b-c)\Delta^t})^{-\frac{c}{b-c}} \quad (15)$$

where  $x^t$ ,  $y^t$  and  $z^t$  represents the number of susceptible, infected and removed individuals in a population of size  $N \in \mathbb{Z}^+$ . In this paper, equations (13-15) will form the basis of the state transition function  $T$  that will be used to formalize the pandemic planning problem as a metric hybrid planning problem  $\Pi$ . Next, we will present the contributions of our paper, namely: (i) the formalization of the pandemic planning problem as a metric hybrid planning problem and (ii) the valid inequalities to help improve the effectiveness of the metric hybrid planner.

## Pandemic Planning Using a Metric Hybrid Planner

In this section, we will demonstrate how the pandemic planning problem can be effectively solved using SCIPPlan.

### The State Transition Model with Lockdowns

We will extend the solution equations of the previously described SIR model to build a state transition function  $T$  with lockdowns. The inputs of function  $T$ , namely the elements of the tuple  $\langle s_1, s_2, s_3, a_1, \Delta \rangle$ , are defined as follows.

- $s_1, s_2, s_3 \in [0, N]$  are the bounded state variables representing the number of susceptible  $x$ , infected  $y$  and removed  $z$  individuals in a population of size  $N$ ,
- $\Delta$  is the fixed duration of a step with the constant value  $\delta \in [\epsilon, M]$ , and
- $a_1 \in \{0, 1\}$  is the binary action variable representing whether the population is under lockdown (i.e.,  $a_1 = 1$ ) or not (i.e.,  $a_1 = 0$ ) over the duration  $\Delta$ .

Similarly, the output of function  $T$  is defined as the tuple of state variables  $\langle s_1, s_2, s_3 \rangle$ . Next, we will modify equations (13-15) with the addition of the binary action variable  $a_1^t$  which will determine the value of the infection rate  $b(a_1)$  over the duration  $\Delta$ . The value of the infection rate  $b(a_1)$  is defined as:

$$b(a_1) = \begin{cases} b_1, & \text{if } a_1 = 1 \\ b_2, & \text{otherwise.} \end{cases} \quad (16)$$

where constants  $b_1, b_2 \in [0, 1]$  represent the infection rates with and without a lockdown, respectively, such that  $b_1 >$

$b_2$ . Given the new definition of the infection rate  $b(a_1)$ , the state transition function  $T$  can be written by symbolically substituting every occurrence of  $x^{t+1}, y^{t+1}, z^{t+1}, x^t, y^t, z^t$  and  $b$  in equations (13-15) with  $s_1^{t+1}, s_2^{t+1}, s_3^{t+1}, s_1^t, s_2^t, s_3^t$  and  $b(a_1)$ , respectively. Next, we will formalize the pandemic planning problem as a metric hybrid planning problem  $\Pi$ .

### The Pandemic Planning Problem

The remaining components of the metric hybrid planning problem  $\Pi$  can be defined to describe the pandemic planning problem as follows.

- $C^T(s_1^t, s_2^t, s_3^t, a_1^t, \Delta^t) \leq 0$  is a constraint on the maximum number of infected individuals allowed at any given time. The temporal constraint enforces that the right-hand side of the state transition function for the state variable  $s_2^{t+1}$  never exceeds the constant threshold  $K \in \mathbb{Z}^+$ . Similarly, the domain of the state variable  $s_2^t$  that represents the number of infected individuals is also bounded by  $K$  such that  $s_2^t \in [0, K]$ .
- $V_1, V_2$  and  $V_3$  are the initial values of the number of susceptible, infected and removed individuals in the population, and are defined as  $V_1 = N - I$ ,  $V_2 = I$  and  $V_3 = 0$  where the constant  $I \in \mathbb{Z}^+$  denotes the initial number of infected individuals.
- $G(s_1^{H+1}, s_2^{H+1}, s_3^{H+1}) \leq 0$  is a constraint on the maximum fraction  $p \in [0, 1]$  of the population that can be removed, and is in the form of:  $s_3^{H+1} \leq pN$ .
- $R(s_1^t, s_2^t, s_3^t, a_1^t, \Delta^t)$  is the reward function that incurs a penalty for a lockdown, and is in the form of:  $-a_1^t$ .

Given the components of  $\Pi$  are defined, SCIPPlan can compile  $\Pi$  into a mathematical optimization model and solve it via constraint generation (i.e., previously described in section ) However, the computational effectiveness of the underlying spatial branch-and-bound solver relies on its ability to effectively derive valid upper and lower bounds on the (nonlinear) expressions that make up the mathematical optimization model (i.e., the objective function (1) and the constraints (2-6)). Therefore, we will next derive valid inequalities in order to improve the computational effectiveness of SCIPPlan.

### Valid Inequalities

In this section, we will introduce domain-dependent valid inequalities in order to improve the computational effectiveness of SCIPPlan. Namely, we will introduce two types of valid inequalities that are based on (i) the monotonicity of state variables  $s_1$  and  $s_3$ , and (ii) the assumption that the size of the population is constant.

1. Monotonic state variables: The analysis of equations (10) and (12) reveals that  $s_1$  is non-increasing and  $s_3$  is non-decreasing.
2. Constant population: The SIR model (Bailey 1975) assumes that the size of the population remains constant.

The monotonicity of state variables and the constant population size assumption are used to define the instantaneous

constraint  $C^I(s_1^t, s_2^t, s_3^t, a_1^t, \Delta^t) \leq 0$  and redefine the goal constraint  $G(s_1^{H+1}, s_2^{H+1}, s_3^{H+1}) \leq 0$ .

### The Mathematical Optimization Model

In this section, we present the mathematical optimization model that is compiled by SCIPPlan to represent and solve the pandemic planning problem.

$$\max_{a_1^1, \dots, a_1^H} \sum_{t=1}^H -a_1^t \quad (17)$$

$$s_1^1 = N - I \quad (18)$$

$$s_2^1 = I \quad (19)$$

$$s_3^1 = 0 \quad (20)$$

$$s_1^{t+1} = s_1^t \left(1 + \frac{s_2^t}{s_1^t}\right)^{e_1} \left(1 + \frac{s_2^t}{s_1^t} e^{e_2}\right)^{-e_1} \quad \forall t \in \{1, \dots, H\} \quad (21)$$

$$s_2^{t+1} = s_2^t \left(1 + \frac{s_2^t}{s_1^t}\right)^{e_1} \left(1 + \frac{s_2^t}{s_1^t} e^{e_2}\right)^{-e_1} e^{e_2} \quad \forall t \in \{1, \dots, H\} \quad (22)$$

$$s_3^{t+1} = N - (s_1^t + s_2^t)^{e_1} (s_1^t + s_2^t e^{e_2})^{-e_3} \quad \forall t \in \{1, \dots, H\} \quad (23)$$

$$s_1^t + s_2^t + s_3^t = N \quad \forall t \in \{1, \dots, H\} \quad (24)$$

$$\left(1 + \frac{s_2^t}{s_1^t}\right)^{e_1} \left(1 + \frac{s_2^t}{s_1^t} e^{(b(a_1) - c)\Delta^t}\right)^{-e_1} \leq 1 \quad \forall t \in \{1, \dots, H\} \quad (25)$$

$$(s_1^t + s_2^t)^{e_1} (s_1^t + s_2^t e^{e_2})^{-e_3} + s_3^t \leq N \quad \forall t \in \{1, \dots, H\} \quad (26)$$

$$s_2^t \left(1 + \frac{s_2^t}{s_1^t}\right)^{e_1} \left(1 + \frac{s_2^t}{s_1^t} e^{e_2}\right)^{-e_1} e^{e_2} \leq K \quad \forall t \in \{1, \dots, H\} \quad (27)$$

$$s_1^{H+1} + s_2^{H+1} + s_3^{H+1} = N \quad (28)$$

$$s_3^{H+1} \leq pN \quad (29)$$

$$s_1^t \in [0, N] \quad \forall t \in \{1, \dots, H+1\} \quad (30)$$

$$s_2^t \in [0, K] \quad \forall t \in \{1, \dots, H+1\} \quad (31)$$

$$s_3^t \in [0, N] \quad \forall t \in \{1, \dots, H+1\} \quad (32)$$

$$a_1^t \in \{0, 1\} \quad \forall t \in \{1, \dots, H\} \quad (33)$$

$$\Delta^t = \delta \quad \forall t \in \{1, \dots, H\} \quad (34)$$

where  $e_1$ ,  $e_2$  and  $e_3$  denote the expressions  $\frac{b(a_1)}{b(a_1) - c}$ ,  $(b(a_1) - c)\Delta^t$  and  $\frac{c}{b(a_1) - c}$ , respectively. The brief description of the resulting mathematical optimization model is as follows. The objective function (17) minimizes the total number of lockdowns used over the horizon. Constraints (18-20) set the initial values of all state variables. Constraints (21-23) represent the state transition function  $T$ . Constraints (24-26) are the valid inequalities that are introduced in section . Constraint (27) is the temporal constraint. Constraints (28-29) are the goal state constraints. Finally, constraints (30-34) specify the domains of state and action variables, and the fixed duration of each step.

## Theoretical Results

In this section, we present our theoretical results on the finiteness and correctness of SCIPPlan for solving the pandemic planning problem with an exponential temporal constraint function  $C^T$ .

**Lemma 1** (Finiteness and correctness of SCIPPlan). *SCIPPlan finds a solution to the pandemic planning problem within some constant  $\gamma > 0$  constraint violation tolerance or proves its infeasibility in finite number of constraint generation iterations.*

*Proof.* We begin our proof with the analysis of equation (14) that governs the evolution of the number of infected individuals  $y$ . The joint analysis of equations (10), (13) and (14) reveals that the expression:

$$(1 + \frac{y^t}{x^t})^{\frac{b}{b-c}} (1 + \frac{y^t}{x^t} e^{(b-c)\Delta^t})^{-\frac{b}{b-c}} \quad (35)$$

is bounded between 0 and 1. This means that the growth of the number of infected individuals  $y$  must be bounded by the expression:

$$K e^{(b-c)\Delta^t} \quad (36)$$

which concludes our proof since expression (36) can be used as the control function in the analysis of the temporal constraint function  $C^T$  instead of the Lipschitz function that was used in the original proof. (Say 2023)  $\square$

## Related Problems and Extensions

In this section, we introduce a modification of the pandemic planning problem that frequently appears in many other areas of social physics, and also show how to extend the pandemic planning problem to use variable step duration. We begin with the presentation of a modification of the pandemic planning problem that frequently appears in other facets of social physics, such as migration, networks and communities. (Jusup et al. 2022) In this new related planning problem, the total cost is primarily made out of two components, namely: (i) the cost associated with the total duration (i.e., makespan) and (ii) the total action duration. In order to solve this new problem, we modify the goal constraint (29) to:

$$s_3^{H+1} \geq qN \quad (37)$$

where  $q \in [0, 1]$  is the minimum fraction  $p \in [0, 1]$  of the population that must reach a certain threshold, and run SCIPPlan with increasing values of horizon  $H$ . For simplicity, we will refer to the previous version of the planning problem as Problem 1, and refer to the new version as Problem 2.

We proceed with the extension of the pandemic planning problem that uses variable step duration. In order to achieve variable step duration, we modify the reward function to:

$$\max_{\substack{a_1^1, \dots, a_1^H \\ \Delta^1, \dots, \Delta^H}} \sum_{t=1}^H -\Delta^t a_1^t \quad (38)$$

Parameter	Values	Brief Description
$b_1$	0.2, 0.25	Infection rate without a lockdown.
$b_2$	0.1, 0.15	Infection rate with a lockdown.
$c$	0.15, 0.2	Removal rate.
$N$	5000	Total population size.
$K$	200, 250	Maximum infected allowed.
$I$	30, 40, 50, 60	Initial infected.
$p$	0.2	Maximum fraction removed.
$q$	0.8	Minimum fraction removed.
$\delta$	14, 21, 28	Fixed duration of a step.
$[\delta_{LB}, \delta_{UB}]$	[7,28]	Variable duration of a step.

Table 1: Summary of the pandemic parameters that are used to create the instances.

and constraint (34) to:

$$\delta_{LB} \leq \Delta^t \leq \delta_{UB} \quad \forall t \in \{1, \dots, H\} \quad (39)$$

where  $\delta_{LB}$  and  $\delta_{UB}$  denote the lower and upper bounds on the duration of each step, respectively.

## Experimental Results

In this section, we present the results of our detailed computational experiments for testing the effectiveness of using SCIPPlan to perform planning under various problem settings.

### Design of Experiments

We have conducted two sets of computational experiments. First, we tested SCIPPlan under both problem settings (i.e., Problem 1 and 2) over 96 instances where each instance corresponds to a unique combination of the parameters provided in Table 1. Second, we tested the effect of using variable step duration on the solution quality and the runtime performance of SCIPPlan.

### Experimental Setup

All experiments were run on the Apple M1 Chip with 16GB memory, using a single thread with one hour total time limit per instance. SCIPPlan uses SCIP (Vigerske and Gleixner 2018) as its spatial branch-and-bound solver.

### Implementation Details

In all of our experiments, we linearized equation (16) using a system of linear constraints. We added the new linearization constraints as a part of the instantaneous constraint  $C^I(s_1^t, s_2^t, s_3^t, a_1^t, \Delta^t) \leq 0$ . We encoded each exponential term of the form  $a^b$  as  $e^{blog(a)}$ . We verified the temporal constraint function  $C^T$  with increments of 0.1.

In order to solve Problem 1 with fixed step duration, we ran SCIPPlan with the value of  $H$  such that  $H\Delta$  is equal to 26 weeks. In order to solve Problem 2 with fixed step duration, we ran SCIPPlan with increasing values of horizon  $H$  until either a solution is found or  $H\Delta$  exceeded 52 weeks. If SCIPPlan returned a solution with  $H\Delta$  that is less than 52 weeks, we verified that the temporal constraint  $C^T(s_1^t, s_2^t, s_3^t, a_1^t, \Delta^t) \leq 0$  holds for the remaining duration of the year without using additional actions (i.e.,  $a_1^t = 0$ ),

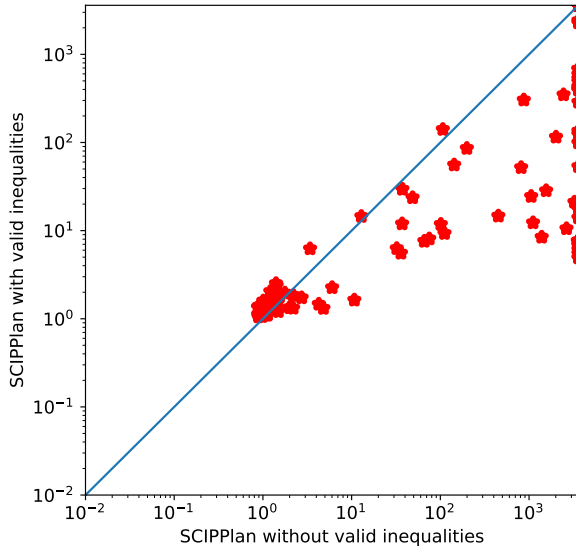


Figure 2: Visualization of the effect of valid inequalities on the logarithmic runtime performance of SCIPPlan in seconds where each data point corresponds to an instance. The addition of the valid inequalities improves the runtime performance of SCIPPlan by around one to two orders of magnitude on average.

otherwise we ran SCIPPlan with the incremented value of  $H$ . Finally, in order to solve Problem 1 with variable step duration, we have used  $\delta_{LB} = 7$  and  $\delta_{UB} = 28$  as the lower and upper bounds of the duration of each step with horizon  $H = 8$ .

### Effect of Valid Inequalities

We begin our analysis with the evaluation of the effect of valid inequalities that are introduced in section (i.e., constraints (24-26)) on the overall runtime performance of SCIPPlan. Figure 2 visualizes the logarithmic runtime comparison between using SCIPPlan with and without the valid inequalities over all instances. In figure 2, each data point represents an instance that corresponds to a unique combination of the parameters provided in Table 1. The inspection of figure 2 clearly highlights the benefit of including the valid inequalities as a part of the planning problems. On average, we observe that the addition of the valid inequalities improves the runtime performance of SCIPPlan by around one to two orders of magnitude. As a result, we report results on the version of the planning problems with the valid inequalities in the remaining of this section.

### Problem Coverage

We proceed with the analysis of our experiments with an overview of the results. Table 2 summarizes the effect of using SCIPPlan to perform planning over both settings with different values of the parameters. Specifically, Table 2

Problem	Parameters	Coverage
1	$b_1 = 0.20, b_2 = 0.10, c = 0.15, K = 200$	12/12
1	$b_1 = 0.20, b_2 = 0.10, c = 0.15, K = 250$	12/12
1	$b_1 = 0.25, b_2 = 0.15, c = 0.2, K = 200$	12/12
1	$b_1 = 0.25, b_2 = 0.15, c = 0.2, K = 250$	12/12
2	$b_1 = 0.20, b_2 = 0.10, c = 0.15, K = 200$	4/12
2	$b_1 = 0.20, b_2 = 0.10, c = 0.15, K = 250$	9/12
2	$b_1 = 0.25, b_2 = 0.15, c = 0.2, K = 200$	11/12
2	$b_1 = 0.25, b_2 = 0.15, c = 0.2, K = 250$	12/12
Total		84/96

Table 2: Summary of the problem coverage grouped by the problem settings and the values of parameters.

groups the total number of instances solved within the time limit for each problem setting and the values of parameters  $b_1$ ,  $b_2$ ,  $c$  and  $K$ , over parameters  $H$  and  $I$ . Overall, we observe that SCIPPlan had the highest success of covering the instances of Problem 1 (i.e., covering all instances). In Problem 2, we observe that SCIPPlan had the highest success of covering the instances with the parameter values  $b_1 = 0.25$ ,  $b_2 = 0.15$  and  $c = 0.2$  (i.e., 23 out of 24 instances), medium success with the parameter values  $b_1 = 0.20$ ,  $b_2 = 0.10$ ,  $c = 0.15$ ,  $K = 250$  (i.e., 9 out of 12 instances), and the lowest success with the parameter values  $b_1 = 0.20$ ,  $b_2 = 0.10$ ,  $c = 0.15$ ,  $K = 200$  (i.e., 4 out of 12 instances). Next, we will inspect both the runtime performance and the normalized solution quality of SCIPPlan over both problem settings.

### Runtime Performance

The runtime performance of SCIPPlan over all unique instances is visualized by figure 3 using heatmaps. The inspection of figure 3 for Problem 1 reveals that decreasing the value of parameter  $\delta$  typically decreases the runtime performance of SCIPPlan, since the lower values of  $\delta$  correspond higher values of horizon  $H$ . The inspection of figure 3 for Problem 2 reveals that decreasing the values of parameters  $\delta$  and  $K$  can significantly decrease the runtime performance of SCIPPlan, since the lower values of  $\delta$  and  $K$  typically correspond to the existence of solutions with higher values of horizon  $H$ . Overall, we have not found a significant effect of the value of parameter  $I$  on the runtime performance of SCIPPlan.

### Normalized Solution Quality

The normalized solution quality of SCIPPlan over all unique instances, that is defined as the total action duration  $\delta \sum_{t=1}^H a_t^t$ , is visualized by figure 4. The inspection of figure 4 highlights the clear benefit of using smaller values of parameter  $\delta$  which allows for a more granular control of the population. In Problem 2, decreasing the value of  $\delta$  by one week decreases the total action duration by around 26 days (i.e., on average). Moreover, we observed that increasing the value of parameter  $K$  can significantly decrease the total action duration. Overall, we have not found a significant effect of the value of parameter  $I$  on the total action duration.

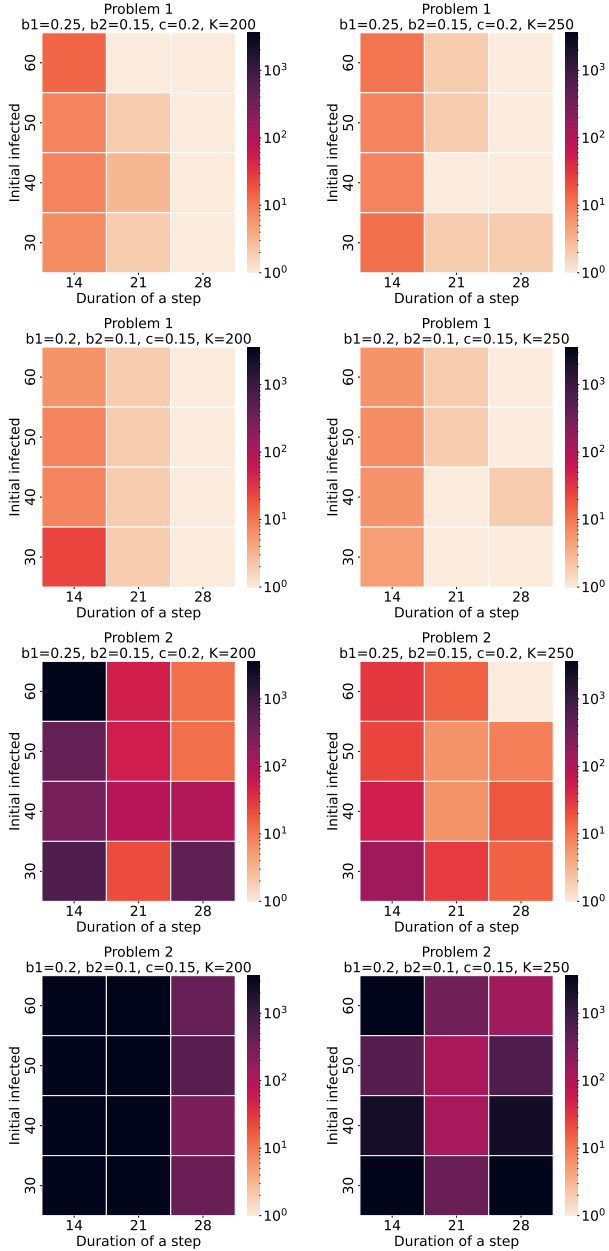


Figure 3: Visualization of logarithmic runtime performance in seconds for both problem settings. Overall, decreasing the value of parameter  $\delta$  typically decreases the runtime performance of SCIPPlan, since the lower values of  $\delta$  correspond higher values of horizon  $H$ .

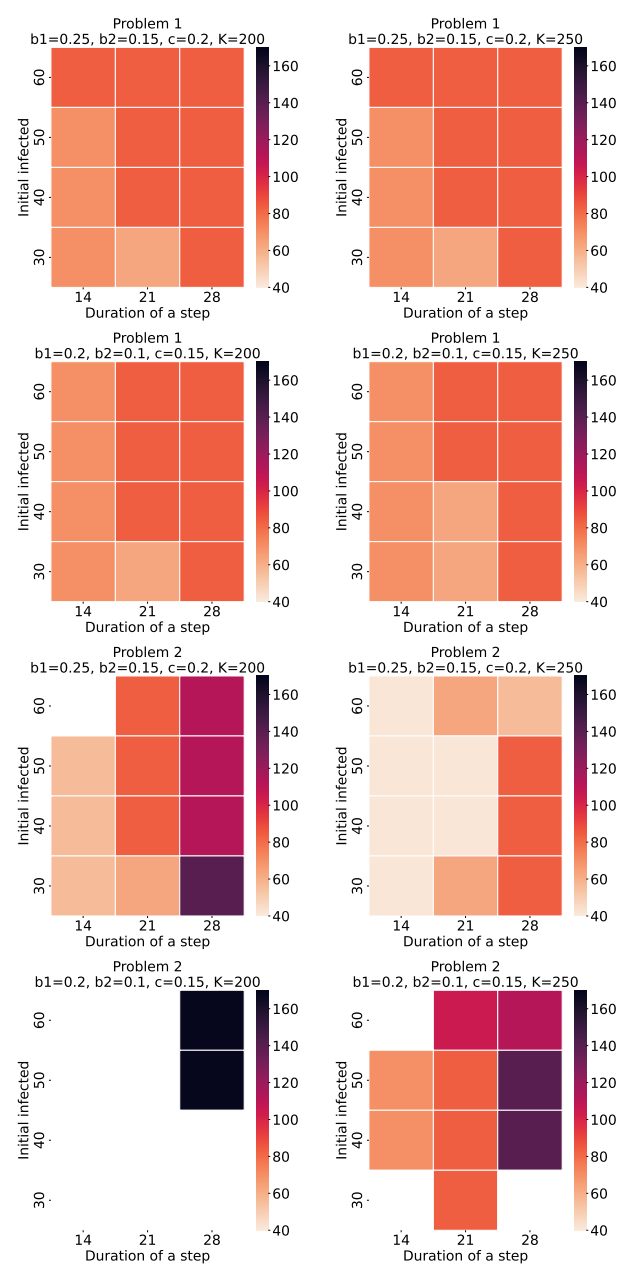


Figure 4: Visualization of total action durations in days for both problem settings. Overall, using smaller values of parameter  $\delta$  increases the solution quality and allows for a more granular control of the population.

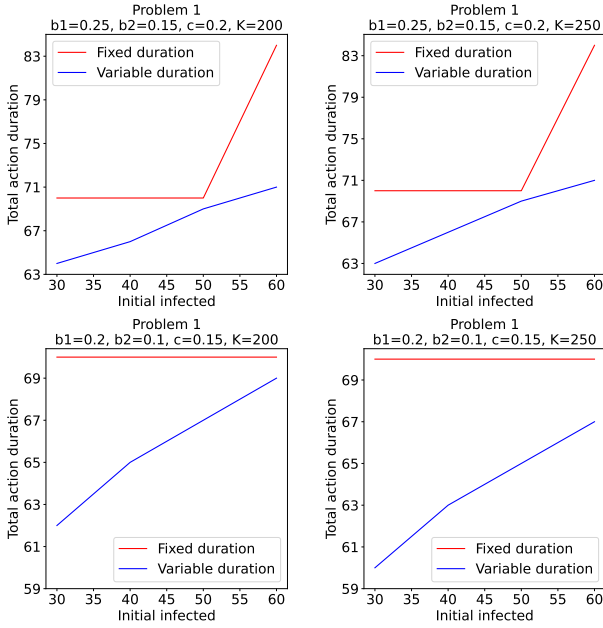


Figure 5: Visualization of total action durations in days over different values of initial infected. The use of the variable step duration over fixed step duration results in higher solution quality (i.e., lower total action duration) in all instances.

### Effect of Using Variable Step Duration

In this section, we analyze the effect of using variable step duration over fixed step duration on the runtime performance and the solution quality of SCIPPlan. In order to achieve this, we ran SCIPPlan with both fixed step duration and variable step duration over all instances of Problem 1.

Figure 5 visualizes the total action duration  $\sum_{t=1}^H \Delta t a_1^t$  comparison between using variable step duration and fixed step duration. The inspection of the figures highlights the clear benefit of using variable step duration over fixed step duration where SCIPPlan finds solutions with higher solution quality (i.e., lower total action duration). However, we have found that the increase in solution quality comes at a price. Figure 6 visualizes the logarithmic runtime comparison between using variable step duration and fixed step duration. On average, we observe that the use of variable step size decreases the runtime performance of SCIPPlan by around two orders of magnitude, which highlights the additional computational resources required to improve the solution quality using variable step duration.

### Discussion and Related Work

In this section, we discuss the importance of our theoretical and experimental results in relation to the literature for the purpose of opening new areas for future work.

In section , we have shown theoretical results on the finiteness and solution quality of SCIPPlan for solving the pandemic planning problem. Our theoretical results yield strong guarantees on the solutions provided by SCIPPlan such that the temporal constraint is satisfied with relatively small val-

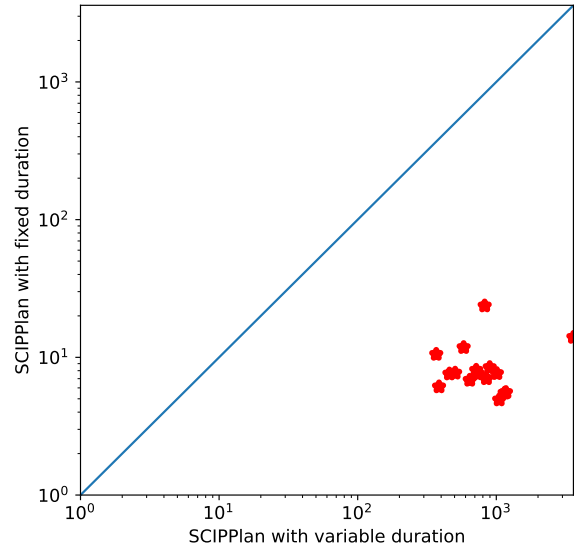


Figure 6: Visualization of the effect of using variable step duration on the logarithmic runtime performance of SCIP-Plan in seconds where each data point corresponds to an instance. The use of the variable step duration decreases the runtime performance of SCIPPlan by around two orders of magnitude on average.

ues of  $\gamma$  where  $\gamma$  is 1.00 for  $K = 200$  and  $\gamma$  is 1.25 for  $K = 250$ .

In section , we have shown the computational performance of our approach to control a pandemic and other related systems. Our experimental results demonstrate the computational benefit of deriving valid inequalities for the planning problem. Some of these valid inequalities (e.g., monotonicity of state variables) are common in many other continuous time decision making problems where the state evolution is governed by a system of partial differential equations. For future work, we plan to investigate the automation of the process of valid inequality derivation for similar metric hybrid planning problems. Further, our experimental results also demonstrate the computational viability of using the exact solution equations of the SIR model (i.e., equations (10- 12)) to construct a nonlinear state transition function  $T$  using both exponential and logarithmic expressions, and perform formal reasoning over continuous time. Our experimental results compliment the success of the existing decision making systems that allow for continuous time decision making under additional restrictive assumptions (e.g., the assumption that the state transition function  $T$  is piecewise linear (Shin and Davis 2005; Coles et al. 2012; Chen, Williams, and Fan 2021), polynomial (Cashmore et al. 2016) etc.). Finally, we highlight the importance of our approach given the availability of machine learning techniques (Raissi, Perdikaris, and Karniadakis 2019; Karniadakis et al. 2021) that can successfully approximate the

solution equations of many systems of partial differential equations using data. For future work, we plan to apply our approach to control a pandemic and other related systems using SCIPPlan based on learned models (Wu, Say, and Sanner 2017; Say and Sanner 2018b; Say, Sanner, and Thiébaut 2019; Say and Sanner 2020; Say et al. 2020; Say 2020; Wu, Say, and Sanner 2020; Say 2021).

## Conclusion

In this paper, we have formalized the pandemic planning problem based on the solution equations of the SIR model and solved it using a metric hybrid planner. We have introduced valid inequalities to improve the runtime effectiveness of the planner. Finally, we have presented both theoretical and experimental results on the performance of our approach to pandemic planning. Overall, we have demonstrated the potential of using metric hybrid planning to help control pandemics and other related systems.

## Ethics Statement

This work studies the computational effectiveness of using the solution equations of a SIR model, and does not constitute as health advice and does not take the place of consulting with the experts of the relevant fields.

## References

Bailey, N. T. J. 1975. *The mathematical theory of infectious diseases and its applications*. Griffin.

Bohner, M.; Streipert, S.; and Torres, D. F. 2019. Exact solution to a dynamic SIR model. *Nonlinear Analysis: Hybrid Systems*, 228–238.

Cashmore, M.; Fox, M.; Long, D.; and Magazzeni, D. 2016. A Compilation of the Full PDDL+ Language into SMT. In *ICAPS*, 79–87.

Chen, J.; Williams, B. C.; and Fan, C. 2021. Optimal mixed discrete-continuous planning for linear hybrid systems. In *Proceedings of the Twenty Fourth International Conference on Hybrid Systems: Computation and Control*, HSCC ’21. Association for Computing Machinery. ISBN 9781450383394.

Coles, A.; Coles, A.; Fox, M.; and Long, D. 2012. COLIN: planning with continuous linear numeric change. *Journal of Artificial Intelligence Research*, 44(1): 1–96.

Gleissner, W. 1988. The Spread of Epidemics. *Applied Mathematics and Computation*, 27(2): 167–171.

Jusup, M.; Holme, P.; Kanazawa, K.; Takayasu, M.; Romić, I.; Wang, Z.; Geček, S.; Lipić, T.; Podobnik, B.; Wang, L.; Luo, W.; Klanjšček, T.; Fan, J.; Boccaletti, S.; and Perc, M. 2022. Social physics. *Physics Reports*, 948: 1–148.

Karniadakis, G. E.; Kevrekidis, I. G.; Lu, L.; Perdikaris, P.; Wang, S.; and Yang, L. 2021. Physics-informed machine learning. *Nature Reviews Physics*.

Kermack, W. O.; and McKendrick, A. G. 1927. A contribution to the mathematical theory of epidemics. *Proceedings of the Royal Society A*.

Li, H. X.; and Williams, B. C. 2008. Generative Planning for Hybrid Systems Based on Flow Tubes. In *Proceedings of the Eighteenth International Conference on Automated Planning and Scheduling*.

McCluskey, T.; and Vallati, M. 2017. Embedding Automated Planning within Urban Traffic Management Operations. In *Proceedings of the International Conference on Automated Planning and Scheduling*, volume 27, 391–399.

Morari, M.; Garcia, C. E.; and Prett, D. M. 1988. Model predictive control: Theory and practice. *IFAC Proceedings Volumes*, 21: 1–12.

Nau, D.; Ghallab, M.; and Traverso, P. 2004. *Automated Planning: Theory & Practice*. San Francisco, CA, USA: Morgan Kaufmann Publishers Inc.

Penna, G. D.; Magazzeni, D.; Mercorio, F.; and Intrigila, B. 2009. UPMurphi: A Tool for Universal Planning on PDDL+ Problems. In *Proceedings of the Nineteenth International Conference on Automated Planning and Scheduling*, ICAPS’09, 106–113. AAAI Press. ISBN 978-1-57735-406-2.

Piotrowski, W.; Fox, M.; Long, D.; Magazzeni, D.; and Mercorio, F. 2016. Heuristic Planning for Hybrid Systems. In *Proceedings of the Thirtieth AAAI Conference on Artificial Intelligence*, AAAI’16, 4254–4255. AAAI Press.

Raissi, M.; Perdikaris, P.; and Karniadakis, G. E. 2019. Physics-informed neural networks: A deep learning framework for solving forward and inverse problems involving nonlinear partial differential equations. *Journal of Computational Physics*, 378: 686–707.

Ramirez, M.; Papasimeon, M.; Lipovetzky, N.; Benke, L.; Miller, T.; Pearce, A. R.; Scala, E.; and Zamani, M. 2018. Integrated Hybrid Planning and Programmed Control for Real Time UAV Maneuvering. In *Proceedings of the 17th International Conference on Autonomous Agents and Multiagent Systems*, AAMAS, 1318–1326. Richland, SC: International Foundation for Autonomous Agents and Multiagent Systems.

Say, B. 2020. *Optimal Planning with Learned Neural Network Transition Models*. Ph.D. thesis, University of Toronto, Toronto, ON, Canada.

Say, B. 2021. A Unified Framework for Planning with Learned Neural Network Transition Models. In *Proceedings of the Thirty-Fifth AAAI Conference on Artificial Intelligence*, 5016–5024.

Say, B. 2023. Robust Metric Hybrid Planning in Stochastic Nonlinear Domains Using Mathematical Optimization. In *Proceedings of the Thirty-Third International Conference on Automated Planning and Scheduling*, ICAPS, 375–383.

Say, B.; Devriendt, J.; Nordström, J.; and Stuckey, P. 2020. Theoretical and Experimental Results for Planning with Learned Binarized Neural Network Transition Models. In *Proceedings of the Twenty-Sixth International Conference on Principles and Practice of Constraint Programming*, 917–934.

Say, B.; and Sanner, S. 2018a. Metric Nonlinear Hybrid Planning with Constraint Generation. In *PlanSOpt 2018*,

19–25. 28th ICAPS Workshop on Planning, Search and Optimization (PlanSOpt).

Say, B.; and Sanner, S. 2018b. Planning in Factored State and Action Spaces with Learned Binarized Neural Network Transition Models. In *Proceedings of the Twenty-Seventh International Joint Conference on Artificial Intelligence*, IJCAI, 4815–4821.

Say, B.; and Sanner, S. 2019. Metric Hybrid Factored Planning in Nonlinear Domains with Constraint Generation. In *Proceedings of the Sixteenth International Conference on the Integration of Constraint Programming, Artificial Intelligence, and Operations Research*, CPAIOR, 502–518.

Say, B.; and Sanner, S. 2020. Compact and Efficient Encodings for Planning in Factored State and Action Spaces with learned Binarized Neural Network Transition Models. *Artificial Intelligence*, 285: 103291.

Say, B.; Sanner, S.; and Thiébaut, S. 2019. Reward Potentials for Planning with Learned Neural Network Transition Models. In Schiex, T.; and de Givry, S., eds., *Proceedings of the Twenty-Fifth International Conference on Principles and Practice of Constraint Programming*, 674–689. Cham: Springer International Publishing.

Say, B.; Wu, G.; Zhou, Y. Q.; and Sanner, S. 2017. Nonlinear Hybrid Planning with Deep Net Learned Transition Models and Mixed-integer Linear Programming. In *Proceedings of the Twenty-Sixth International Joint Conference on Artificial Intelligence*, IJCAI, 750–756.

Scala, E.; Haslum, P.; Thiébaut, S.; and Ramírez, M. 2016. Interval-Based Relaxation for General Numeric Planning. In *ECAI*, 655–663.

Shin, J.-A.; and Davis, E. 2005. Processes and Continuous Change in a SAT-based Planner. *Artificial Intelligence*, 166(1-2): 194–253.

Thiébaut, S.; Coffrin, C.; Hijazi, H.; and Slaney, J. 2013. Planning with MIP for Supply Restoration in Power Distribution Systems. In *Proceedings of the Twenty-Third International Joint Conference on Artificial Intelligence*, 2900–2907.

Vigerske, S.; and Gleixner, A. 2018. SCIP: Global Optimization of Mixed-Integer Nonlinear Programs in a Branch-and-cut Framework. *Optimization Methods and Software*, 33(3): 563–593.

Wu, G.; Say, B.; and Sanner, S. 2017. Scalable Planning with Tensorflow for Hybrid Nonlinear Domains. In *Proceedings of the Thirty-First International Conference on Neural Information Processing Systems*, NIPS, 6276–6286. USA: Curran Associates Inc.

Wu, G.; Say, B.; and Sanner, S. 2020. Scalable Planning with Deep Neural Network Learned Transition Models. *Journal of Artificial Intelligence Research*, 68: 571–606.